Catalysis Letters Vol. 109, Nos. 3–4, July 2006 (© 2006)
DOI: 10.1007/s10562-006-0078-y

Reaction kinetics and intermediate determination of solid acid catalysed liquid-phase hydrolysis reactions: a real-time *in situ* ATR FT-IR study

Gerben M. Hamminga,* Guido Mul and Jacob A. Moulijn

Reactor & Catalysis Engineering, Delft University of Technology, Julianalaan 136, 2628 BL Delft, The Netherlands

Received 1 February 2006; accepted 7 March 2006

The appearance of catalyst–reactant interactions observed in on-line ATR FT-IR spectra of Nafion/silica catalysed esterification and etherification reactions of 1-octanol was investigated. It was assessed by variation of catalyst and solvent that the catalyst–reactant band is a result of the reaction of silica with 1-octanol, yields Si–O–R functionalities. Based on off-line TPD-MS and TGA characterisation of the used solid catalyst powder, the formation of Si–O–R linkages on the SiO_2 surface was confirmed. This demonstrates conclusively that in specific liquid-phase reactions, on-line analysis of intermediate species adsorbed on heterogeneous catalysts is possible. Using on-line particle analyzers, it was assessed that the absorptions were not the result of severe attrition of the catalyst particles in the course of the reaction, but apparently the result of apolar interactions of the particles with the diamond crystal.

KEY WORDS: Nafion/silica catalyst; esterification; etherification; real-time *in situ* ATR FT-IR spectroscopy; heterogeneous catalysis.

1. Introduction

Attenuated total reflection (ATR) Fourier transform infrared spectroscopy (FT-IR) as real-time *in situ* monitoring tool, has proven its applicability in various disciplines of (fine) chemical and chemical engineering research. For the development of new synthesis routes and processes for pharmaceutical products, ATR FT-IR was successfully applied as real-time *in situ* tool to elucidate reaction mechanisms and kinetics [1, 2]. Also for the development of pharmaceutical crystallisation processes, for which the kinetics of crystal growth and nucleation are of great importance, this technique has proven to be most valuable for the determination of supersaturation concentrations [3–6].

In polymer research this real-time *in situ* technique also showed to be an excellent monitoring tool, as reactions can be analysed without complicated reactor modifications or expensive deuterated monomers in order to reveal the reaction kinetics and mechanism [7–15].

In catalysis research, e.g. homogeneous catalysis, with this technique not only kinetic and mechanistic information was obtained, but also information about the internal co-ordination of the applied metal complex to the substrate [16–30]. Although in polymer and catalysis research mostly organic phases are being studied, also in aqueous phases e.g. in biocatalysis research, ATR spectroscopy has shown considerable potential as novel method for on-line measurements of biocatalytic conversions [31].

In heterogeneous catalysis, this technique is extensively used to study adsorbed surface species on thin film layers deposited on an internal reflection element (IRE), which is mostly a gas-phase application. Only few papers on real-time *in situ* ATR FT-IR spectroscopy have been dedicated to kinetic and mechanistic studies of heterogeneous liquid-phase catalytic reactions at relative low pressures [32–37]. In these studies, however, no evidence was found of reactants, reaction intermediates or products interacting with or adsorbed on the catalyst surface. E.g. Pintar et al. report that, within the applied operating window (298 or 308 K, 1 or 10 bara), no influence of catalyst particles dispersed in the liquid-phase was found on the collected ATR FT-IR spectra [36].

In a previous publication we have applied real time *in situ* ATR FT-IR spectroscopy for analysis of the esterification and etherification reactions of 1-octanol and hexanoic acid (see figure 1) using Nafion/silica catalysts, with the main result being the appearance of IR bands in the spectra that were tentatively assigned to interactions of one the reactants (alcohol) with the solid catalyst particles [35]. The present study aims to further evaluate the nature of the intermediate species adsorbed on the heterogeneous catalysts, and the reason behind the appearance of the accompanying absorptions in the ATR-spectra, including particle size effects.

*To whom correspondence should be addressed.
E-mail: G.M.Hamminga@tnw.tudelft.nl

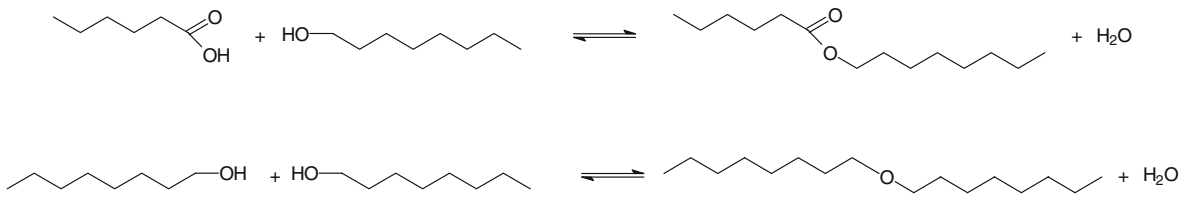

Figure 1. Esterification and etherification reaction analysed in the present study.

2. Experimental

2.1. Materials

Both the esterification reaction of hexanoic acid (95 + %, Merck) and 1-octanol (95 + %, Baker) and the etherification reaction of 1-octanol were performed in a reflux slurry configuration, as was reported in [35]. The kinetics of both reactions was either studied in cumene (98%, Acros) at 427 K, or in *n*-decane (95 + %, Merck) at 447 K. The pressure was atmospheric, the total reaction volume was 200 ml containing 0.4 mol/l acid and alcohol, and 1.0 g of a Nafion on silica composite consisting of 13% w/w Nafion, respectively. A sieve fraction of 35–75 μm of the Nafion composite catalyst was applied, which was kindly provided by Dupont (N_2-BET area typically 350 m^2/g). In experiments where silica was added, Silica gel Davisil™ grade 643 (99 + % Aldrich), was used, in a somewhat smaller sieve fraction (35–53 μm, N_2-BET area of 300 m^2/g).

2.2. Kinetic measurements

For a typical experiment at first, the glass reactor was filled with solvent after which hexanoic acid and the catalyst were added. Next, 1-octanol was added to the reaction mixture when the reflux temperature was reached, which is the starting point of the reaction and collection of FT-IR spectra. In the case of studying the etherification a mixture of solvent and catalyst was heated to reflux temperature, followed by 1-octanol addition.

The ATR FT-IR equipment used for on-line reaction monitoring and the apparatus applied for "off-line" GC-analysis have been described in detail in a previous publication [35]. Also the processing of the obtained ATR-spectra is described in this publication.

2.3. Analysis of particle size distributions

For the investigation of particle dimensions and population a Lasentec FBRM D600R in-process probe was used, which was obtained from Mettler Toledo. This probe has a tip diameter of 25 mm and a sapphire window that can withstand pressures up to 10 bar and temperatures between −90 and 300 °C. Particle sizes in the range of 0.5 μm–2.5 mm can be detected in scan intervals of at least 2 s. The applied conditions depend mainly on the solvent used.

The applied probe employs the focused beam reflectance (FBR) principle. This principle is based on the backscattering of a focused laser beam, which follows a circular path in the liquid-phase. When a particle is passing through this focused beam it will start to backscatter the laser light until the opposite end of the particle is reached (see figure 2). The distance measured is the chord length. By applying this method typically tens of thousands of chord lengths per second can be measured. The constructed chord length distribution

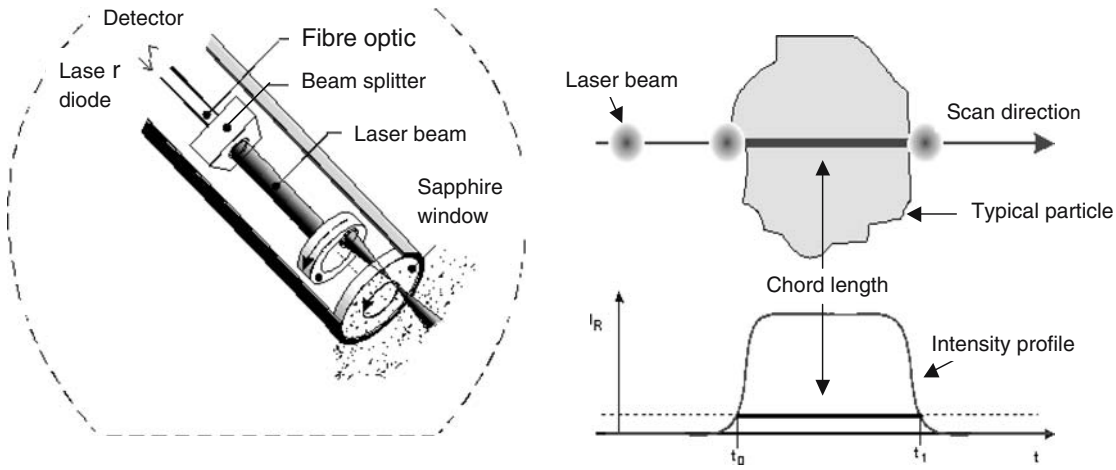

Figure 2. FBRM probe and chord length measurement. Adapted from [38].

gives a highly precise and sensitive means of observing changes in both particle dimensions and particle population [38].

2.4. TGA and TPD-MS analysis

To investigate the nature of chemisorbed species at the catalyst surface both Thermogravimetric Analysis (TGA) and TPD-MS were applied. For the TGA analysis a TGA/SDTA851^e thermobalance, equipped with a TSO 801RO sample robot and a TSO 800GC1 gas control unit was used (All obtained from Mettler Toledo). Helium was applied as a carrier gas in all experiments, and fed with a flow rate of 100 ml/min. Samples of approximately 25 mg were heated at a constant rate of 10 K per minute, to a final temperature of 1073 K. Desorption of chemisorbed reaction species present on the catalyst carrier was studied by TPD-MS using an atmospheric plug-flow reactor. Approximately 35.2 mg of sample was weighed into a quartz TPD reactor. After assembly of the reactor in the set-up, a helium flow of 50 ml/min (maximal flow rate) was applied over the reactor bed. When a stable MS-signal was obtained (after half an hour), the reactor was heated to 1073 K at a heating rate of 10 K per min.

3. Results

3.1. Reaction kinetics

The main region (1250–1000 cm^{-1}) obtained from on-line ATR FT-IR monitoring of the esterification reaction in cumene (at 427 K) and *n*-decane (at 447 K) that is of interest for the reaction kinetics is already extensively discussed in [35]. Therefore, in this study we only want to focus on the second region of interest (1250–1000 cm^{-1} region) that is illustrated in figure 3, which is the region where 1-octanol, ester and an unknown reaction product shows IR absorptions. As is illustrated in this figure, the asymmetric C–O stretching frequency of 1-octanol can be detected (1045 cm^{-1} at 427 K). Figure 3 also shows the production of the ester at 1170 cm^{-1}, which is assigned to the asymmetric C–O stretching frequency. Besides the bands assigned to the ester and alcohol, a very strong IR band was observed at 1100 cm^{-1}. The observation of this band is the basis of this study in order to elucidate the origin of this band.

3.2. Observation of catalyst interactions

The further investigation of the band dynamics of the unknown compound has been reported in a previous publication [35]. The results of this investigation are summarized in figure 4, and illustrate the effects of the difference in reaction temperature and reaction mixtures on the dynamics of the band at 1100 cm^{-1}.

As illustrated by figure 4, during the esterification reaction in *n*-decane this band was not observed at all (curve A (•) in figure 4). In the experiment in decane, where no acid was present in the reaction medium, only a relative low intensity of the 1100 cm^{-1} band was obtained. In cumene, even in the presence of the esterification reaction, the increase in the absorption band was observed, which is significantly enhanced in the absence of acid (curve E). Only without Nafion on the catalyst carrier, a more rapid formation of the band at 1100 cm^{-1} was observed in *n*-decane (curve F).

The emerging 1100 cm^{-1} absorbance band was further investigated, as was reported in [35], by comparing ATR-spectra were taken from both silica particles and Nafion on silica particles (both without solvent). The ATR-spectra obtained from both solids show a broad band of SiO_2 between 1120 and 1020 cm^{-1} that is assigned to Si–O–Si stretching vibrations, and the weak

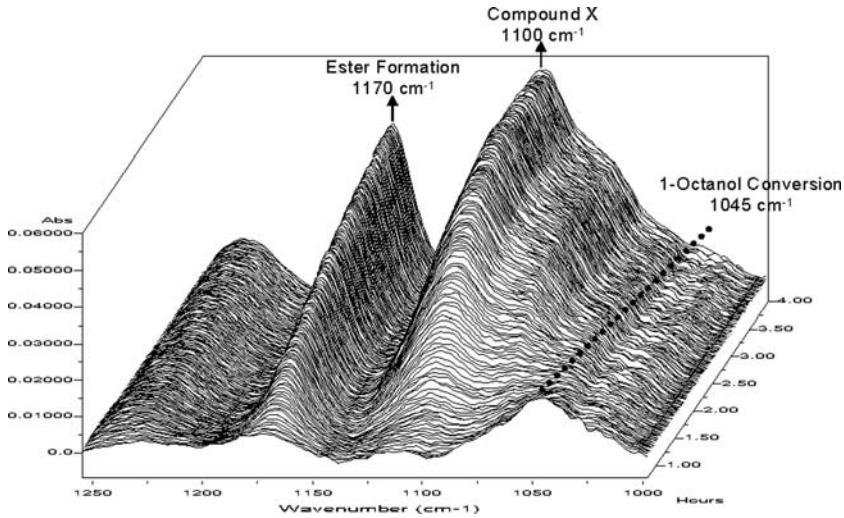

Figure 3. Real-time FT-IR waterfall plot of the 1250–1000 cm^{-1} region collected in cumene. Dynamics of absorption frequencies of 1-octanol, ester, and unknown compound X, respectively. Conditions: 200 ml, 0.4 mol/l 1-octanol , 0.4 mol/l hexanoic acid, 1.0 g Nafion/Silica at 427 K.

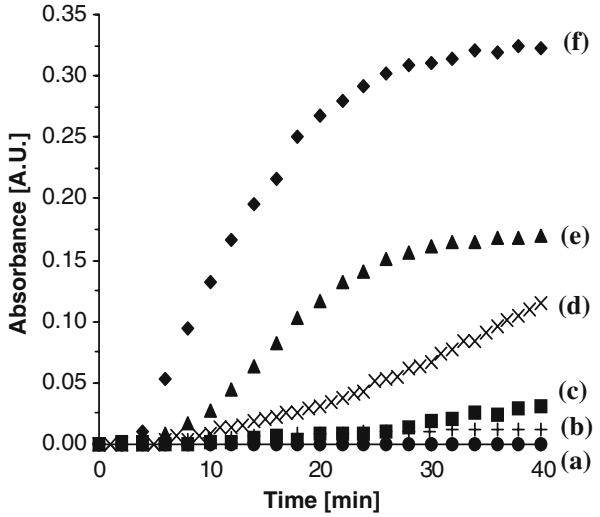

Figure 4. Comparison of the 1100 cm^{-1} band dynamics under various conditions: (A, ●) esterification in *n*-decane (447 K); (B, +) esterification in *n*-decane (427 K); (C, ■) etherification of 1-octanol in *n*-decane (447 K); (D, ×) esterification in cumene (427 K, figure 3); (E, ▲) etherification of 1-octanol in cumene (427 K); (F,◇) reaction of 1-octanol with silica in *n*-decane (447 K).

band at around 975 cm^{-1} to Si–O–H [39–42]. The IR bands assigned to SiO_2 particles are near the wavenumbers observed in the on-line spectra. Moreover, when comparing the wavenumbers of the unknown compound with spectra published in open literature indicate that the absorption band at around 1100 cm^{-1} should be assigned to the formation of alkoxy linkages of 1-octanol to the silica surface. The asymmetric and symmetric stretching vibrations of alkoxy groups (Si–O–C) are located at 1100 cm^{-1} ((C–O)M stretching) and 800 cm^{-1}. The CH_2-wag absorbance band of the Si–O–R surface group is typically found at 1260 cm^{-1} [39–42]. Whether the origin of the 1100 cm^{-1} absorbance band is really caused by Si–O–R surface groups associated with SiO_2 particles rather than with dissolved alkoxy species, was further investigated by conducting a filtration experiment of the reaction of 1-octanol with silica in *n*-decane, as is reported in [35]. This experiment strongly suggests that the high intensity bands at 1100 cm^{-1} in the spectra are vibrations related to SiO_2 particles associated with alkoxy species.

3.3. *Investigation of the origin of vibrations assigned to alkoxy-linkages*

3.3.1. *Effect of catalyst attrition*

The possibility of the formation of small silica particles during reaction (i.e. catalyst attrition) was investigated by means of on-line particle size measurements. The most severe absorbance in the on-line ATR-FT-IR measurement is expected from particle sizes of, at least the size of the penetration depth of the evanescent wave into the sample. The penetration depth of the evanescent wave can be calculated with the following formula [43]:

$$d_p = \frac{\lambda}{4 \cdot \pi \cdot n_1 \cdot \left[\sin^2\theta - \left(\frac{n_2}{n_1}\right)^2\right]^{\frac{1}{2}}}. \quad (1)$$

In which d_p is the penetration depth in nm, λ is the wavelength in nm, n_1 is the refractive index of diamond, n_2 is the refractive index of the reaction mixture (in this case the refractive index of the solvent is taken; cumene: 1.491, *n*-decane 1.411), and θ is the angle of incidence of the infrared light (in this case 45°). As the refractive index of diamond is depending on the wavelength of the infrared light, a Herzberger-type dispersion equation was used to calculate the refractive index of diamond [44].

$$n_2 = A + B \cdot L + C \cdot L^2 + D \cdot \lambda^2 + E \cdot \lambda^4. \quad (2)$$

In which $L = 1/(\lambda^2 - 0.028)\lambda$ in μm, and $A = 2.3755$, $B = 3.3644 \cdot 10^{-2}$, $C = -8.8752 \cdot 10^{-2}$, $D = -2.4046 \cdot 10^{-6}$, and $E = 2.2139 \cdot 10^{-9}$.

By applying both formulas 1 and 2 the maximal penetration depths in cumene and *n*-decane can be determined. At 650 cm^{-1} (15.385 μm) the estimated penetration depth in cumene and *n*-decane were approximately 0.904 and 0.852 μm, respectively. Thus, the on-line particle size measurements give information on the presence, or formation of particle sizes of below 1 μm during the reaction. For these measurements an insertion probe was used.

To investigate whether catalyst attrition could be inducing the 1100 cm^{-1} absorbance band, chord length distributions were measured of catalyst particles applied in the esterification at 427 K in cumene and at 447 K in *n*-decane, respectively. The ATR-spectra obtained were consistent with the results reported in [35] for cumene at 427 K and for *n*-decane at 447 K. The resulting chord length distributions are depicted in figure 5A, B. The chord length distribution for the esterification reaction at 427 K in cumene is given in figure 5A. At the end of the reaction a small but significant shift in the chord length distribution has occurred indicating that de-agglomeration of catalyst particles has occurred. The end curve shows no formation of fines indicating that attrition of catalyst particles is limited.

Figure 5B depicts the chord length distribution for the esterification at 447 K in *n*-decane. This experiment shows the same trend in chord length distribution as was obtained for the experiment at 427 K in cumene. In this case also some agglomerates were present at the start of the reaction. Despite of the fact that de-agglomeration had occurred no fines were observed during the course of the esterification reaction under these conditions. It must be noted that in both experimental cases catalyst particle sizes below 1 μm were not present neither in the beginning of the experiment nor at the end. Also no influence of bigger particles/agglomerates were found on

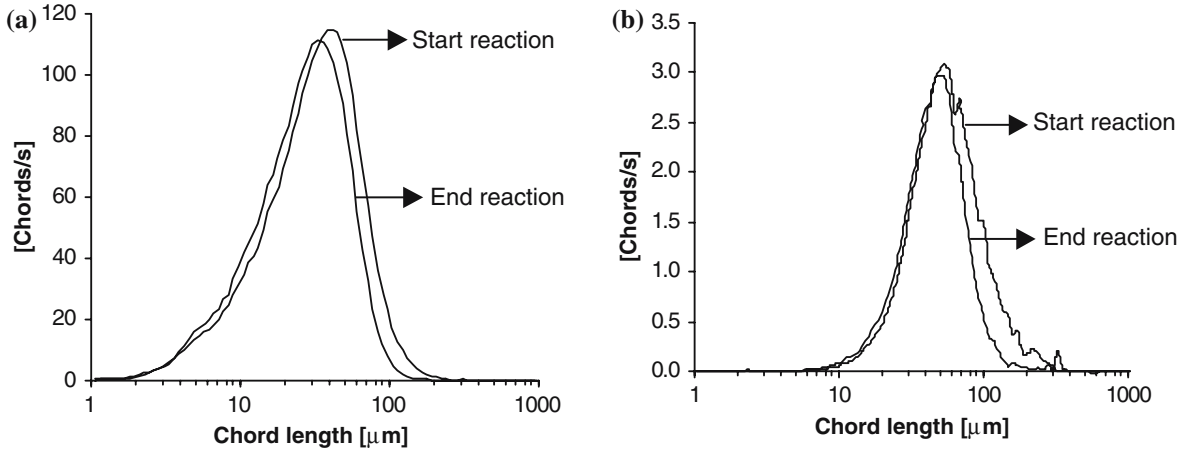

Figure 5. (A) Chord length distributions of Nafion/silica catalyst particles at the start and end of the esterification reaction in cumene at 427 K. Conditions: 200 ml, 0.4 mol/l 1-octanol, 0.4 mol/l hexanoic acid, 1.0 g Nafion/Silica at 427 K. (B) Chord length distributions of Nafion/silica catalyst particles at the start and end of the esterification reaction in *n*-decane at 447 K. Conditions: 200 ml, 0.4 mol/l 1-octanol, 0.4 mol/l hexanoic acid, 1.0 g Nafion/Silica at 447 K. Spectra were not corrected for solvent, 1-octanol, and catalyst.

the successive ATR spectra, as no absorbance bands of catalyst particles were observed just before addition of 1-octanol.

3.3.2. TGA and TPD-MS

In order to validate whether physisorbed or chemisorbed 1-octanol is causing the very strong 1100 cm^{-1} absorbance band in the ATR-spectra, TGA analysis was applied on the Nafion/silica catalyst (as received), the spent Nafion/silica catalyst after 3 h of reaction in a mixture containing cumene, hexanoic acid and 1-octanol at 427 K (case D in figure 4) and silica particles applied in a reaction mixture of *n*-decane and 1-octanol at 447 K after 3 h of reaction (case F. in figure 4).

Figure 6(A–C) depicts the derivative profiles of the TGA results obtained for the three cases.

In the case of the Nafion/silica catalyst (as received), figure 6A, between 323 and 398 K physisorbed residual water is evaporated. In the interval of 523–723 K SO_2 evolution is observed, which is caused by decomposition of the SO_3^- group of the Nafion resin. At around 773 K several decomposition products like, HF, and SiF_4 are observed. The obtained TGA results are in good agreement with the results described in literature [45, 46].

In the derivative profile of Nafion/silica catalyst used in the esterification reaction in cumene at 427 K (figure 6B), besides the evolution of water in the interval between 323 and 398 K also the evaporation of cumene is observed at around 427 K. Like in the case of the unused Nafion/silica catalyst the production of SO_2 is detected in the interval from 523 to 723 K, although the evolution temperatures have somewhat shifted. The decomposition band assigned to HF and SiF_4 at around 773 K has broadened, which indicates the presence of an additional decomposing species.

The broadening of the decomposition band at around 773 K, in the case of the spent Nafion/silica catalyst, was compared to a TGA profile of silica particles reacted in *n*-decane at 447 K in the presence of 1-octanol. The resulting derivative profile is depicted in figure 6C, which shows the presence of some water and solvent. However, at around 573 K the evolution is detected of a species believed to be related to a $Si–O–C_8H_{17}$ like chemisorbed compound that maximises at around 773 K. This confirms the result found for the spent catalyst, indicating the presence of an additional chemisorbed species (besides HF and SiF_4) on the catalyst carrier surface at around 773 K.

The desorption experiment for silica particles reacted in *n*-decane at 447 K in the presence of 1-octanol was repeated in a set-up combining TPD and mass spectrometry (TPD-MS).

At 773 K, where the desorption rate of the chemisorbed species is maximising, the following mass spectrum was recorded (see figure 7). The numbers in figure 7 indicate the most important mass fractions. Reference spectra of 1-octanol and dioctyl ether are shown in figure 8. In both figure 8A, B the most important mass fractions are indicated by the numbers.

Comparing the mass fractions in figures 8A, B for 1-octanol and dioctyl ether with the obtained mass spectrum of the desorbed compound in figure 7, the mass fraction pattern in figure 8A strongly resembles the mass fractions pattern obtained for the desorbed compound in figure 7. On the other hand, the mass fraction pattern of dioctyl ether (figure 8B) significantly differs from the mass fraction pattern in figure 7, especially in the mass fractions 43, 57, and 71. This indicates a very low concentration of dioctyl ether on the catalyst surface, if any, and the absence of ether formation during the desorption step.

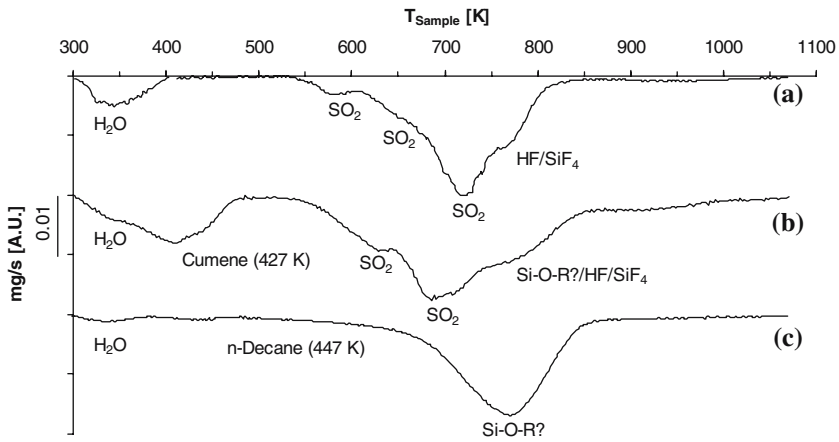

Figure 6. (A) TGA derivative profile of Nafion/Silica as received (19.7 mg). TGA conditions: 100 ml/min He, heating rate of 10 K/min. (B) TGA derivative profile of spent Nafion/Silica (23.6 mg) reacted for 3 h in a cumene, hexanoic acid, 1-octanol mixture under conditions as described in figure 5A. 1100 cm^{-1} band dynamics as described in figure 4D. TGA conditions: 100 ml/min He, heating rate of 10 K/min. (C) TGA derivative profile of silica (34.4 mg). Reaction conditions: 1 g silica reacted for 3 h at 447 K in a *n*-decane (200 ml), 1-octanol (0.4 mol/l). 1100 cm^{-1} band dynamics as described in figure 4F. TGA conditions: 100 ml/min He, heating rate of 10 K/min.

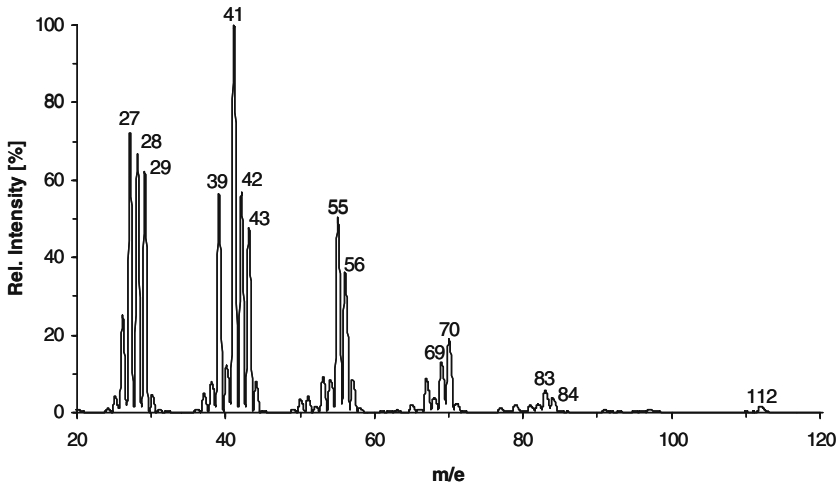

Figure 7. Mass spectrum of chemisorbed surface species evolved from silica particles (1 g) reacted in *n*-decane (200 ml) at 447 K in the presence of 1-octanol (0.4 mol/l), 1100 cm^{-1} band dynamics as described in figure 4F. TPD conditions: 35.2 mg of sample, 50 ml/min He, heating rate of 10 K/min. Mass spectrum obtained at TPD temperature of 773 K.

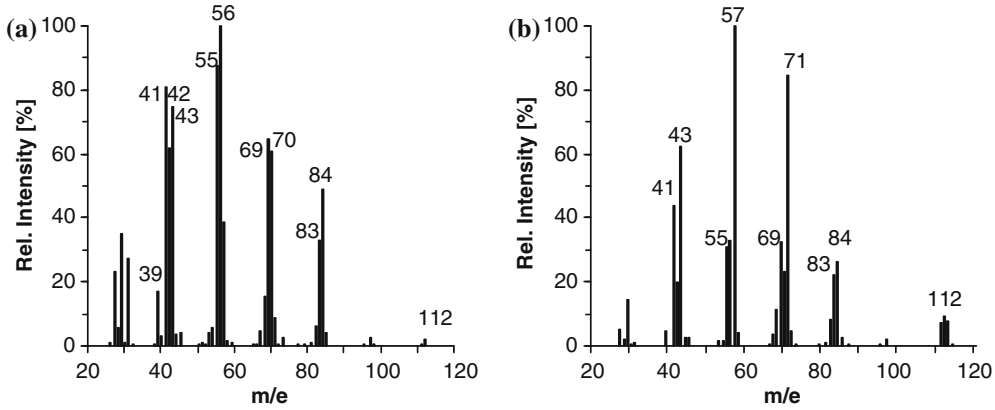

Figure 8. (A) Mass spectrum of 1-octanol. (B) Mass spectrum of dioctyl ether.

4. Discussion

4.1. In situ reaction monitoring

ATR FT-IR is a very useful technique to analyse heterogeneously catalysed esterification reactions, its kinetics, and reaction mechanism. Complementary results with the off-line analysis are obtained when studying the reaction kinetics, since the obtained concentration profiles by on-line reaction monitoring are in perfect agreement with GC-analysis [35]. The fact that the analysis is performed during the reaction allows the observation of short living, or labile, intermediates. Either in the vials used for GC-analysis, or on the GC columns, these intermediates will have decomposed before they can be analysed. The ability of on-line reaction monitoring to detect reaction intermediates is illustrated by the fact that an intermediate is observed during the esterification at 427 K in cumene (figure 4D), whereas this intermediate was not observed when changing the reaction temperature to 447 K in *n*-decane (figure 4A). Being able to detect these intermediates provides valuable information on the mechanism for this reaction, as this intermediate was not detected by GC-analysis.

Numerous other advantages of the *in situ* monitoring are obvious. Especially the fact that samples do not have to be extracted from the reactor is highly advantageous if one wants to determine reaction kinetics. Artefacts due to volume changes are prevented this way.

It should be mentioned here, that the formation of a Si–O–R species (at 1100 cm^{-1}) on the catalyst surface severely interferes with both the analyses of side product formation (ether) and the 1-octanol reactant, in the case of the esterification reaction.

4.2. Catalyst–reactant interactions

The experimental work in our previous publication [35] provide us with evidence that the band dynamics of the Si–O–R absorbance frequencies can be ascribed to the visibility of particles, and not Si–O–R species desolved in the reaction medium.

Particle size measurements indicate the absence of fines at the beginning and the end of the esterification reaction in both cumene and *n*-decane (figure 5A, B). It should be mentioned however that, in the case of the esterification in cumene, a significant amount of particles in the range of 2–10 μm was present in the reaction mixture. Despite the presence of these small particles during the reaction, SiO_2 related vibration bands were not observed. This is probably because the size of these particles still exceeds the maximal penetration depth ($\asymp$1 μm) of the evanescent wave. As the production of fines during the esterification reaction was not observed, the 1100 cm^{-1} band is most certainly not caused by attrition of the silica carrier.

Several studies on interactions of adsorbed alcohol species, such as methanol, ethanol and 2-propanol, on silica surfaces been reported in literature. The adsorption of methanol on silicalite and silica surfaces was studied by Pelmenschikov et al. [45, 47], whereas Natal-Santiago et al. studied the adsorption of methanol and ethanol on silica [45, 48]. Both studies applied transmission FT-IR spectroscopy to investigate surface interactions of the adsorbed species. Poston et al. applied ATR FT-IR spectroscopy to study adsorbed 2-propanol at the silica surface on a silica-coated ZnSe internal reflection element. Though intense interactions of the alcohols were observed in these studies, strong Si–O–R adsorption bands in the 1100 cm^{-1} region were not reported [43, 45]. In the present study, by conducting TGA (figure 6C) experiments in a Helium atmosphere of silica particles that had reacted in a mixture of *n*-decane and 1-octanol (figure 4F), the desorption of a chemisorbed species at around 773 K was detected, believed to originate form Si–O–C_8H_{17} surface species. This should be compared with physisorbed 1-octanol on silica, which is expected to desorb at around 468 K (boiling point of 1-octanol). Re-examination of the "reacted" silica particles under the same conditions in a TPD-MS set-up confirmed the presence of these surface species, since the mass fraction pattern of this compound nicely coincides with the mass fraction pattern of 1-octanol (see figure 7, 8A).

Normally, specific strong interactions of the silica and adsorbed surface species to ATR internal reflection elements are established by means of coating an internal reflection element. For example Rivera et al. and Poston et al. applied silica suspensions in ethanol to dip-coat a Germanium reflection element [43, 49], also high-surface-area silica particles combined with a polymeric binder have been applied to coat ZnSe reflection elements [50].

The present study indicates that also in particular cases with immersion probes, the interactions of chemisorbed species on the surface silica particles can be observed without the use of coating procedures.

5. Conclusions

In situ ATR FT-IR spectroscopy utilising the ATR sampling technique is a powerful analysis tool for monitoring heterogeneous catalytic hydrolysis reactions. Not only excellent results have been obtained when comparing conventional off-line GC-analysis with the on-line measurements, but also the reaction kinetics determined by both techniques, are in agreement. The surplus value of the *in situ* technique was illustrated by the fact that interactions with catalyst particles were observed in both hydrolysis reactions, which could not be detected by GC-analysis. However, off-line GC-analysis was still required to determine reaction selectivity due to the severe interference of the absorbance bands of the observed intermediates.

Further evaluation of the observed reaction intermediate indicated that this compound associated with the 1100 cm^{-1} vibration band was related to catalyst particles, as when the particles were filtered off the 1100 cm^{-1} band disappeared. By conducting on-line particle size measurements during the esterification reaction it was shown that no fines were present or produced during the reaction. No evidence was found of particle sizes present in the reaction mixture interfering with the evanescent wave of ATR FT-IR spectroscopic technique, indicating that the observed intermediate was not caused by the catalyst carrier alone.

Finally by investigating the catalyst carrier after reaction utilising TGA and TPD-MS, the observed reaction intermediate could be characterised as being 1-octanol chemisorbed on the catalyst carrier as a Si–O–C_8H_{17} surface species. This indicates that in this specific case catalyst surface species can be observed when utilising ATR FT-IR spectroscopy in heterogeneous catalysed liquid-phase reactions, predominantly if the rates of formation of these species is significantly higher than subsequent reaction leading to the final products.

Acknowledgments

Mettler Toledo is gratefully acknowledged for making the FBRM-equipment available and for operational support for this equipment. Avantium Technologies is acknowledged for financial support.

References

[1] G.J. Dozeman, P.J. Fiore, T.P. Puls and J.C. Walker, Org. Proc. Res. Dev. 1 (1997) 137.
[2] T.J.N. Watson, S.W. Horgan, R.S. Shah, R.A. Farr, R.A. Schnettler, C.R. Nevill Jr, F.J. Weiberth, E.W. Huber, B.M. Baron, M.E. Webster, R.K. Mishra, B.L. Harrison, P.L. Nyce, C.L. Rand and C.T. Goralski, Org. Proc. Res. Dev. 4 (2000) 477.
[3] D.D. Dunuwila and K.A. Berglund, J. Crystal Growth 179 (1997) 185.
[4] G. Févotte, Int. J. Pharm. 241 (2002) 263.
[5] R. Tamura, D. Fujimoto, Z. Lepp, K. Misaki, H. Miura, H. Takahasi, T. Ushio, T. Nakai and K. Hirotsu, J. Am. Chem. Soc. 124 (2002) 13139.
[6] T. Togkalidou, H.-H. Tung, Y. Sun, A. Andrews and R.D. Braatz, Org. Proc. Res. Dev. 6 (2002) 317.
[7] H. Hua and M.A. Dubé, J. Polym. Sci. Part A: Polym. Chem. 39 (2001) 1860.
[8] R. Jovanovic and M.A. Dubé, J. Appl. Poly. Sci. 82 (2001) 2958.
[9] B. Kappler, A. Tuchbreiter, D. Faller, P. Liebetraut, W. Horbelt, J. Timmer, J. Honerkamp and R. Mülhaupt, Polymer 44 (2003) 6179.
[10] S. Maier, T. Loontjens, B. Scholtens and R. Mülhaupt, Macromolecules 36 (2003) 4727.
[11] A.J. Pasquale and T.E. Long, Macromolecules 32 (1999) 7954.
[12] A.J. Pasquale, R.D. Allen and T.E. Long, Macromolecules 34 (2001) 8064.
[13] J.E. Puskas and M.G. Lanzendörfer, Macromolecules 31 (1998) 8684.
[14] J.E. Puskas, M.G. Lanzendörfer and W.E. Pattern, Polym. Bull. 40 (1998) 55.
[15] R.F. Storey and T.L. Maggio, Macromolecules 33 (2000) 681.
[16] M. Allmendinger, R. Eberhardt, G. Luinstra and B. Rieger, J. Am. Chem. Soc. 124 (2002) 5646.
[17] S. Denmark and S.M. Pham, Helv. Chim. Acta 83 (2000) 1846.
[18] S.E. Denmark and J. Fu, J. Am. Chem. Soc. 122 (2000) 12021.
[19] J.E. Ellis, E.M. Davis, G.J. Dozeman, E.A. Lenoir, D.T. Belmont and P.L. Brower, Org. Proc. Res. Dev. 5 (2001) 226.
[20] C. Gaul, P.I. Arvidsson, W. Bauer, R.E. Gawley and D. Seebach, Chem. Eur. J. 7 (2001) 4117.
[21] M. Grabarnick and S. Zamir, Org. Proc. Res. Dev. 7 (2003) 237.
[22] N.S. Josephsohn, K.W. Kuntz, M.L. Snapper and A.H. Hoveyda, J. Am. Chem. Soc. 123 (2001) 11594.
[23] S. Kainz, A. Brinkmann, W. Leitner and A. Pfaltz, J. Am. Chem. Soc. 121 (1999) 6421.
[24] T.R. Kelly, R.A. Silva and G. Finkenbeiner, Tetrahedon Lett. 41 (2000) 9651.
[25] R.G. Konsler, J. Karl and E.N. Jacobsen, J. Am. Chem. Soc. 120 (1998) 10780.
[26] J.R. McConnell, K.P. Barton, M.A. LaPack and M.A. DesJardin, Org. Proc. Res. Dev. 6 (2002) 700.
[27] A. Pintar, J. Batista and J. Levec, Analyst 127 (2002) 1535.
[28] C.H. Senanayake, G.B. Smith, K.M. Ryan, L.E. Fredenburgh, J. Liu, F.E. Roberts, D.L. Hughes, R.D. Larsen, T.R. Verhoeven and P.J. Reider, Tetrahedon Lett. 37 (1996) 3271.
[29] A. Thompson, E.G. Corley, M.F. Huntington, E.J.J. Grabowski, J.F. Remenar and D.B. Collum, J. Am. Chem. Soc. 120 (1998) 2028.
[30] J.R. Zoeller, N.L. Buchanan, T.J. Dickson and K.K. Ramming, Catal. Today 49 (1999) 431.
[31] M.R. Dadd, D.C.A. Sharp, A.J. Pettman and C.J. Knowles, J. Microbio. Meth. 41 (2000) 69.
[32] R.M. Dyson, M. Hazenkamp, K. Kaufmann, M. Maeder, M. Studer and A. Zilian, J. Chemometrics 14 (2000) 737.
[33] C. LeBlond, J. Wang, R. Larsen, C. Orella and Y.-K. Sun, Top. Catal. 5 (1998) 149.
[34] B.H. Lipshutz, S. Tasler, W. Chrisman, B. Spliethoff and B. Tesche, J. Org. Chem. 68 (2003) 1177.
[35] G. Mul, G.M. Hamminga and J.A. Moulijn, Vib. Spectrosc. 34 (2004) 109.
[36] A. Pintar, R. Malacea, C. Pinel, G. Fogassy and M. Besson, Appl. Catal. A – Gen. 264 (2004) 1.
[37] J. Weitkamp, M. Hunger and U. Rymsa, Micropor. Mesopor. Mater. 48 (2004) 255.
[38] J. Worlitschek, T. Redman, H. Briggeler, O. Ubrich, P. Barrett, B. O'Sullivan and C. Didierjean, AutoChem. (2005) 1.
[39] J. Guilment, O. Poncelet, J. Rigola and S. Truchet, Vib. Spectrosc. 11 (1996) 37.
[40] K.A. Mauritz and R.M. Warren, Macromolecules 22 (1989) 1730.
[41] G.D. Soraru, F. Babonneau, C. Gervais and N. Dallabona, J. Sol-Gel Sci. Technol. 18 (2000) 11.
[42] N.B. Colthup, L.H. Daly and S.E. Wiberley, *Introduction to Infrared and Raman Spectroscopy* (Academic Press, San Diego, 1990) 358.
[43] P.E. Poston, D. Rivera, R.H. Uibel and J.M. Harris, Appl. Spectrosc. 52 (1998) 1391.
[44] D.F. Edwards and E. Ochoa, J. Opt. Soc. Am. 71 (1981) 607.
[45] Q. Deng, C.A. Wilkie, R.B. Moore and K.A. Mauritz, Polymer 39 (1998) 5961.
[46] S.R. Samms, S. Wasmus and R.F. Savinell, J. Electrochem. Soc. 143 (1996) 1498.
[47] A.G. Pelmenschikov, G. Morosi, A. Gamba, A. Zecchina, S. Bordiga and E.A. Paukshtis, J. Phys. Chem. 97 (1993) 11979.
[48] M.A. Natal-Santiago and J.A. Dumesic, J. Catal. 175 (1998) 252.
[49] D. Rivera, P.E. Poston, R.H. Uibel and J.M. Harris, Anal. Chem. 72 (2000) 1543.
[50] B.J. Ninness, D.W. Bousfield and C.P. Tripp, Appl. Spectrosc. 55 (2001) 655.